

See discussions, stats, and author profiles for this publication at: <https://www.researchgate.net/publication/7704055>

Ellipsometric and Neutron Diffraction Study of Pentane Physisorbed on Graphite

ARTICLE *in* LANGMUIR · SEPTEMBER 2005

Impact Factor: 4.46 · DOI: 10.1021/la050338c · Source: PubMed

CITATIONS

21

READS

19

7 AUTHORS, INCLUDING:



Ulrich Volkmann

Pontifical Catholic University of Chile

98 PUBLICATIONS 666 CITATIONS

[SEE PROFILE](#)



Haskell Taub

University of Missouri

159 PUBLICATIONS 2,204 CITATIONS

[SEE PROFILE](#)



K. W. Herwig

Oak Ridge National Laboratory

131 PUBLICATIONS 1,251 CITATIONS

[SEE PROFILE](#)

Ellipsometric and Neutron Diffraction Study of Pentane Physisorbed on Graphite

Frank Kruchten,[†] Klaus Knorr,[†] Ulrich G. Volkmann,[‡] Haskell Taub,^{*,§}
Flemming Y. Hansen,[‡] Blake Matthies,^{§,#} and Kenneth W. Herwig^{§,#}

Technische Physik, Universität des Saarlandes, D 66041 Saarbrücken, Germany, Facultad de Física, Pontificia Universidad Católica de Chile, Santiago 22, Chile, Department of Physics and Astronomy and University of Missouri Research Reactor, University of Missouri-Columbia, Columbia, Missouri 65211, and Department of Chemistry, Technical University of Denmark, IK 207 DTU, DK-2800 Lyngby, Denmark

Received February 5, 2005

High-resolution ellipsometry and neutron diffraction measurements have been used to investigate the structure, growth, and wetting behavior of fluid pentane ($n\text{-C}_5\text{H}_{12}$) films adsorbed on graphite substrates. We present isotherms of the thickness of pentane films adsorbed on the basal-plane surfaces of a pyrolytic graphite substrate as a function of the vapor pressure. These isotherms are measured ellipsometrically for temperatures between 130 and 190 K. We also describe neutron diffraction measurements in the temperature range 11–140 K on a deuterated pentane ($n\text{-C}_5\text{D}_{12}$) monolayer adsorbed on an exfoliated graphite substrate. Below a temperature of 99 K, the diffraction patterns are consistent with a rectangular centered structure. Above the pentane triple point at 143.5 K, the ellipsometric measurements indicate layer-by-layer adsorption of at least seven fluid pentane layers, each having the same optical thickness. Analysis of the neutron diffraction pattern of a pentane monolayer at a temperature of 130 K is consistent with small clusters having a rectangular-centered structure and an area per molecule of $\sim 37 \text{ \AA}^2$ in coexistence with a fluid monolayer phase. Assuming values of the polarizability tensor from the literature and that the monolayer fluid has the same areal density as that inferred for the coexisting clusters, we calculate an optical thickness of the fluid pentane layers in reasonable agreement with that measured by ellipsometry. We discuss how these results support the previously proposed “footprint reduction” mechanism of alkane monolayer melting. In the hypercritical regime, we show that the layering behavior is consistent with the two-dimensional Ising model and determine the critical temperatures for layers $n = 2\text{--}5$.

I. Introduction

The wetting behavior of fluid films of normal alkanes [$n\text{-C}_n\text{H}_{2n+2}$] has been the subject of only a small number of investigations. In the case of shorter alkanes that are largely of fundamental interest, there have been detailed studies of multilayer ethane (C_2H_6) films adsorbed on graphite to determine the layer condensation critical temperatures by the volumetric adsorption isotherm technique¹ and by high-resolution ellipsometry.² In the case of longer alkanes ($15 \leq n \leq 50$), which have greater technological interest,³ there have been studies of the wetting topologies of fluid films adsorbed on SiO_2 surfaces.^{4–8} These alkanes are of sufficient length to exhibit the surface freezing effect at the bulk liquid/air

interface.⁹ For these longer alkanes, wetting of the fluid film on the SiO_2 surface occurs a few degrees above the bulk triple point.

In this paper, we use ellipsometry and neutron diffraction to investigate the structure and growth of fluid pentane ($n\text{-C}_5\text{H}_{12}$) films adsorbed on a graphite basal-plane surface. Although not so long an alkane as to exhibit the surface freezing effect, pentane is long enough for the flexibility of its carbon backbone to play a role in the structure of the fluid film. Our two experimental techniques are complementary in that the solid monolayer structure can be probed by neutron diffraction where the pressure is too low for ellipsometric measurements. On the other hand, neutron diffraction is ineffective for investigating the structure of multilayer fluid films that have relatively broad diffraction peaks. In this regime, the layering behavior is more easily investigated by ellipsometry that has sufficient resolution to observe practically vertical steps in vapor pressure adsorption isotherms corresponding to the growth of successive film layers.

II. Methods and Materials

A. Ellipsometry. The thickness of pentane ($n\text{-C}_5\text{H}_{12}$) films physisorbed on the basal-plane surfaces of graphite was measured by high-resolution ellipsometry as a function of the vapor pressure for temperatures between 130 and 190 K. The ellipsometry instrumentation is described in more detail elsewhere.¹⁰ To

* Author to whom correspondence should be addressed.

[†] Universität des Saarlandes.

[‡] Pontificia Universidad Católica de Chile.

[§] University of Missouri-Columbia.

[‡] Technical University of Denmark.

[#] Present address: The Goodyear Tire and Rubber Co., Corporate Research Division, Akron, OH 44305.

Present address: Spallation Neutron Source, Oak Ridge National Laboratory, Oak Ridge, TN 37830.

(1) Regnier, J.; Menaucourt, J.; Thomy, A.; Duval, X. *J. Chim. Phys.* **1981**, *78*, 629.

(2) Nham, H. S.; Hess, G. B. *Phys. Rev. B* **1988**, *38*, 5166.

(3) See, e.g.: Xia, T. K.; Ouyang, J.; Ribarsky, M. W.; Landman, U. *Phys. Rev. Lett.* **1992**, *69*, 1967.

(4) Merkl, C.; Pfohl, T.; Riegler, H. *Phys. Rev. Lett.* **1997**, *79*, 4625.

(5) Holzwarth, A.; Leporatti, S.; Riegler, H. *Europhys. Lett.* **2000**, *52*, 653.

(6) Schollmeyer, H.; Ocko, B.; Riegler, H. *Langmuir* **2002**, *18*, 4351.

(7) Volkmann, U. G.; Pino, M.; Altamirano, L. A.; Taub, H.; Hansen, F. Y. *J. Chem. Phys.* **2002**, *116*, 2107.

(8) Mo, H.; Taub, H.; Volkmann, U. G.; Pino, M.; Ehrlich, S. N.; Hansen, F. Y.; Lu, E.; Miceli, P. *Chem. Phys. Lett.* **2003**, *377*, 99.

(9) Earnshaw, J. C.; Hughes, C. J. *Phys. Rev. A* **1992**, *46*, R4494. Wu, X. Z.; Sirota, E. B.; Sinha, S. K.; Ocko, B. M.; Deutsch, M. *Phys. Rev. Lett.* **1993**, *70*, 958. Wu, X. Z.; Ocko, B. M.; Sirota, E. B.; Sinha, S. K.; Deutsch, M.; Cao, B. H.; Kim, M. W. *Science* **1993**, *261*, 1018.

(10) Volkmann U. G.; Knorr, K. *Surf. Sci.* **1989**, *221*, 379.

summarize it briefly, a monochromator-grade pyrolytic graphite crystal is embedded in a copper block that is in turn mounted on the coldfinger of a closed-cycle refrigerator.¹¹ This ensures that the graphite substrate is the coldest point in the ultrahigh-vacuum chamber that has a base pressure less than 10^{-10} mbar. In addition to an opening for passage of the ellipsometer's laser light, the block has a hole to allow light from a pulsed Nd:YAG laser beam to be scanned over the graphite sample for cleaning purposes.

The adsorbate vapor was admitted to the chamber at roughly a constant rate such that the pressure increased to the bulk vapor pressure at the given temperature in about 2 h. Capacitance gauges (Baratron) and a spinning ball viscosimeter were used to measure the vapor pressure of the pentane, which had a nominal purity of 99.6% (Fluka) and which was further purified by distillation. During its growth, the film's optical thickness, t , increases in proportion to the change, $\delta\Delta$, of the phase delay, Δ , between the electric field components parallel and perpendicular to the reflection plane. As such, t is proportional to both the coverage, θ (the number of molecules above a unit area on the surface), and the effective polarizability of the molecules, which depends on their orientation with respect to the substrate.

B. Neutron Diffraction. The neutron scattering experiments were carried out on a two-axis diffractometer equipped with a five-counter multidetector/acquisition system located at C-port of the University of Missouri Research Reactor.¹² The substrate consisted of a stack of about 90 disks of exfoliated graphite (Grafoil¹³) having a specific surface area of ~ 24 m²/g as determined by a nitrogen vapor pressure isotherm.¹⁴

Alkane monolayers were deposited from the vapor phase introduced through a capillary tube to the Grafoil cell.¹⁵ The pentane was 98% deuterated as supplied.¹⁶ It was purified by pumping on it during repeated freeze/thaw cycles. The diffraction experiments were performed at wavelengths of 4.33 and 1.27 Å in a transmission geometry with the plane of the Grafoil disks parallel to the horizontal scattering plane.^{17,18} A neutron diffraction pattern took about 3 days to record. Background diffraction patterns from the bare graphite substrate were obtained at two temperatures, 11 and 100 K. For each diffraction pattern taken with the pentane present, the background pattern closest in temperature was subtracted. Below room temperature, the temperature gradient across the sample was less than 3 K. The diffraction patterns were analyzed using a profile-analysis technique that yields structural parameters such as the monolayer unit cell, the molecular orientation, and the monolayer coherence length, as has been described elsewhere.^{19,20}

III. Results

A. Ellipsometry. In Figure 1, we show a series of adsorption isotherms in the liquid regime $T > T_t$ where $T_t = 143.46$ K is the triple point of pentane. For each temperature, the ellipsometric thickness, t , is plotted vs reduced vapor pressure, p/p_0 , where p_0 is the saturated vapor pressure. All of the isotherms have the shape expected for layer-by-layer growth, showing steps and plateaus corresponding to growth of successive layers. Each isotherm terminates in a *bona fide* infinitely thick film, demonstrating complete wetting at the saturated

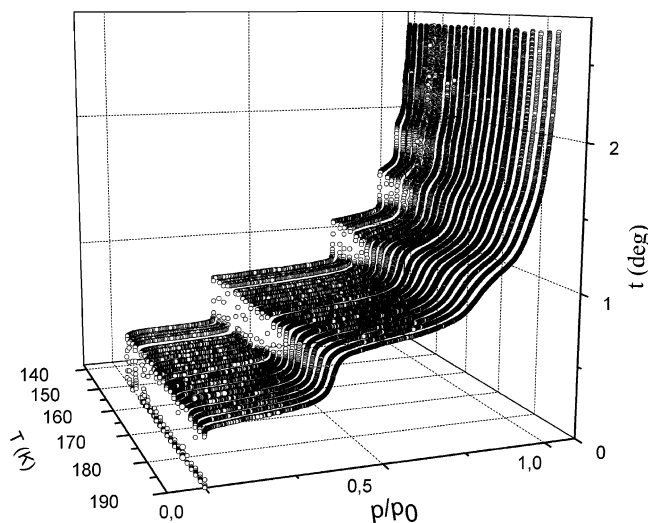


Figure 1. A series of adsorption isotherms (ellipsometric thickness, t , as a function of the relative vapor pressure, p/p_0) in the fluid regime of pentane on graphite.

vapor pressure, p_0 , corresponding to bulk coexistence. At the lowest temperatures, seven or eight steps are observed. They are practically vertical, suggesting that the formation of each layer can be interpreted as a first-order layering transition such that at step n there is coexistence between n layers on part of the surface and $n - 1$ layers on the remaining part. For steps $n = 2, 3, 4, 5$, there is a critical temperature $T_c(n)$ above which the step is no longer vertical. Below, we evaluate these critical temperatures.

The first layer forms at a pressure so low that it could only be measured with the spinning ball viscosimeter. Due to the finite sampling time of the gauge and the delicate adjustment of the needle valve in the gas inlet, only a few points could be obtained near the first step in the isotherm. This precludes a detailed analysis of this feature.

From the ellipsometric isotherms, we can obtain the layering pressures, p_n , from the points of steepest slope on the steps and the optical film thickness, t_n , at the completion of the n th layer from the midpoint of the plateaus. For all temperatures included in Figure 1, we find that, to a good approximation, t_n increases linearly with the number of steps, n , as shown in Figure 2 for $n = 1-7$. This corresponds to an average phase shift per layer $\langle \Delta t_n \rangle = 0.388^\circ \pm 0.002^\circ$ for the first seven steps where $\Delta t_n \equiv \delta\Delta_n - \delta\Delta_{n-1}$. We find no systematic variation in the values of Δt_n to within the indicated uncertainty. Therefore, as the layer number n increases, any decrease in the molecular density within a layer must be compensated by an increase in the effective molecular polarizability. This might occur, for example, if the long axis of the pentane molecules in the upper fluid layers begins to tilt toward the surface normal or if there are conformational changes of the molecule which increase its polarizability. We note that a layer thickness independent of n differs from that found previously in ellipsometry measurements on the rare gases argon, krypton, and xenon.²¹ For these films, the layer density decreased monotonically as n increased. However, as in the case of the rare gas studies, no temperature dependence of the rare gas layer thickness was observed.

B. Neutron Diffraction. In Figure 3, we show the neutron diffraction pattern obtained at a wavelength of

(11) Kruchten, F. Ph.D. thesis, Technische Physik, Universität des Saarlandes, 2004.

(12) Berliner, R.; Mildner, D. F.; Sudol, J.; Taub, H. In *Position Sensitive Detection of Thermal Neutrons*; Convert, P., Forsyth J. B., Eds.; Academic Press: New York, 1983; p 120.

(13) UCAR Carbon Co., P.O. Box 94637, Cleveland, OH 44101.

(14) Wang, S.-K.; Newton, J. C.; Wang, R.; Taub, H.; Dennison, J. R.; Shechter, H. *Phys. Rev. B* **1989**, *39*, 10331.

(15) Herwig, K. W.; Newton, J. C.; Taub, H. *Phys. Rev. B* **1994**, *50*, 15287.

(16) Cambridge Isotope Laboratories, 50 Frontage Road, Andover, MA 01810.

(17) Herwig, K. W.; Matthies, B.; Taub, H. *Phys. Rev. Lett.* **1995**, *75*, 3154.

(18) Matthies, B. Ph.D. thesis, University of Missouri-Columbia, 1999.

(19) Trott, G. J. Ph.D. thesis, University of Missouri-Columbia, 1981.

(20) Trott, G. J.; Taub, H.; Hansen, F. Y.; Danner, H. R. *Chem. Phys. Lett.* **1981**, *78*, 504.

(21) Faul, J. W. O.; Volkmann, U. G.; Knorr, K. *Surf. Sci.* **1990**, *227*, 390.

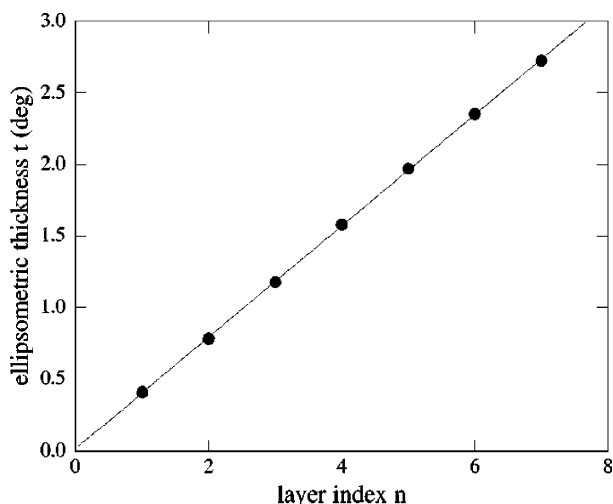


Figure 2. Optical film thickness at the completion of the n th layer, t_n , as a function of layer index, n . The same average phase shift per layer $\langle \Delta t_n \rangle = 0.388^\circ \pm 0.002^\circ$ was obtained for all temperatures in Figure 1.

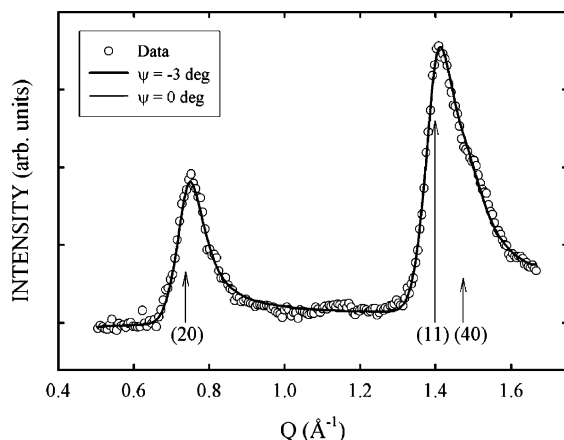


Figure 3. Diffraction pattern of a 1.01-layer film of deuterated pentane ($n\text{-C}_5\text{D}_{12}$) adsorbed on Grafoil obtained with a neutron wavelength of 4.33 Å. The same diffraction profile (solid curve) is calculated for the unit cell in Figure 4 with either $\psi = 0^\circ$ or -3° .

4.33 Å from a 1.01-layer deuterated pentane film ($n\text{-C}_5\text{D}_{12}$) adsorbed on the Grafoil substrate at a temperature of 11 K. At this wavelength, the diffraction pattern contains three Bragg peaks which can be indexed as the (20), (11), and (40) reflections, respectively, of a rectangular unit cell. Assuming close packing, the area of this cell is large enough to contain two molecules. The solid curve is the diffraction profile calculated for a rectangular-centered (RC) structure corresponding to the unit cell shown in Figure 4 with the in-plane azimuthal angle, ψ , between the long molecular axis and the a lattice vector set to zero. Both molecules in the cell are assumed to be in the all-trans configuration with the plane of their carbon skeleton parallel to the graphite surface. The height of the vertical arrows above the Miller indices indicates the relative intensity calculated for the three Bragg peaks. The (40) peak appears only as a weak shoulder on the high- Q side of the dominant (11) peak. The fit represented by the solid curve in Figure 3 gives lattice constants $a = 17.01$ Å and $b = 4.67$ Å with an uncertainty of ± 0.02 Å. We estimate the uncertainty in the azimuthal angle ψ is $\pm 5^\circ$. This estimate is based on diffraction profiles calculated for the rectangular unit cell in Figure 4 with $\psi = 0^\circ$, -3° , and -4.7° which are virtually indistinguishable. The profiles for $\psi = 0^\circ$ and -3° are shown in Figure 3.

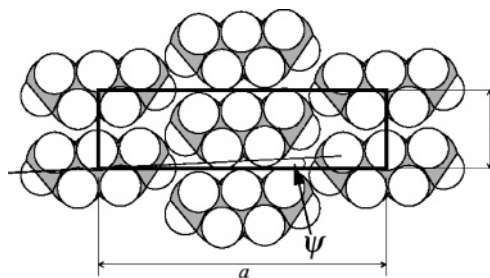


Figure 4. Unit cell of the pentane monolayer on graphite at a temperature of 11 K. The molecules are in the all-trans configuration with the plane of their carbon skeleton parallel to the surface. ψ is the angle between the long axis of molecule and the a lattice vector.

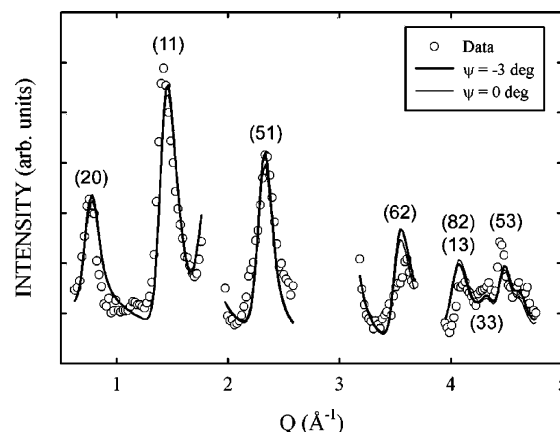


Figure 5. Diffraction pattern of a 1.01-layer film of deuterated pentane ($n\text{-C}_5\text{D}_{12}$) adsorbed on Grafoil obtained with a neutron wavelength of 1.27 Å. The diffraction profiles calculated for the unit cell in Figure 4 with $\psi = -3^\circ$ (thick line) and 0° (thin line) are nearly identical.

To corroborate the low-temperature pentane monolayer structure shown in Figure 4, we also obtained a neutron diffraction pattern at 11 K using a shorter neutron wavelength of 1.27 Å, as shown in Figure 5. This pattern contains a larger number of Bragg peaks and hence potentially provides further constraints on a structural model. However, it also contains Q ranges (where no data points appear in Figure 5) in which background subtraction cannot be performed reliably due to intense Bragg peaks of the graphite substrate. In practice, we found it necessary to fix the a lattice constant to the value determined from the longer wavelength diffraction pattern in order to fit the observed (20) peak position. In Figure 5, we see that diffraction profiles calculated for $\psi = -3^\circ$ (thick line) and 0° (thin line) are nearly identical. We also fit a model in which the ψ angles of the two molecules in the rectangular unit cell of Figure 4 have the same magnitude ($\psi = 3^\circ$) but opposite sign. This staggered two-sublattice model does not have the full herringbone (HB) symmetry because the symmetry of the pentane molecule in Figure 4 only allows one of the two glide lines required (the one along the b direction, but not the one along a). It provides as good a fit as the calculated profiles in Figure 5, whereas we obtain a worse fit with the model having the full HB symmetry obtained by rotating one of the molecules in the unit cell by 180° about its long axis.

We compared both the RC and HB structures with those calculated by minimizing the potential energy of a monolayer cluster of pentane molecules on a smooth graphite surface (no corrugation) as described in ref 15. These calculations assumed a rectangular unit cell with the a and b lattice constants fixed at their experimentally

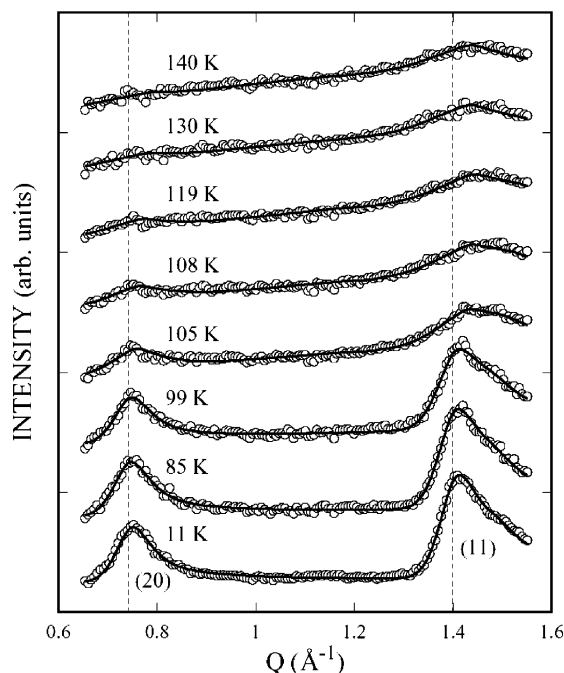


Figure 6. Temperature dependence of the diffraction patterns from a 1.01-layer film of deuterated pentane ($n\text{-C}_5\text{D}_{12}$) adsorbed on Grafoil. Neutron wavelength is 4.33 Å. The solid curve is the best fit to each diffraction pattern.

determined values. They favored neither an RC nor a staggered structure (i.e., different ψ angles were obtained for the two molecules in the unit cell) but did yield small values for $|\psi| < 6^\circ$.¹⁸

Arnold et al.²² inferred an RC unit cell with $\psi = 0$ for a pentane submonolayer on graphite from their X-ray and neutron diffraction measurements at temperatures below 50 K. However, their neutron diffraction pattern does not extend above $Q = 3 \text{ Å}^{-1}$ so that they were unable to access the (62) and (53) Bragg peaks. Our larger Q range allows a better test of an HB structure, a possibility that they did not consider.

In Figure 6, we show neutron diffraction patterns as a function of temperature taken with the longer neutron wavelength of 4.33 Å. There is no detectable change in the diffraction patterns up to a temperature of 99 K. Between 99 and 105 K, there is a large increase in the width of the two Bragg peaks and a shift of their position to higher wave vector transfer Q . We interpret this behavior as indicating the melting of the pentane monolayer in this temperature range. The intensity that remains in the diffraction peaks at temperatures above 99 K suggests considerable short-range order in the fluid phase of the pentane monolayer. To investigate this possibility, we have fit the diffraction pattern in Figure 6 at 130 K to an RC structure ($\psi = 0$) but allowed the coherence length, L , to vary in the calculation of the diffraction profile.^{19,20} This analysis yields lattice constants of $a = 16.0 \text{ Å}$ and $b = 4.57 \text{ Å}$, corresponding to an area per molecule of 36.6 Å^2 . From the width of the leading edge of the diffraction peaks,²³ we estimate a monolayer coherence length $L \approx 26 \text{ Å}$ at 130 K compared to $L \approx 77 \text{ Å}$ at 11 K. As found in previous molecular dynamics simulations of butane and hexane monolayers,²⁴ we interpret these results as indicating the presence of small monolayer clusters coexisting with a

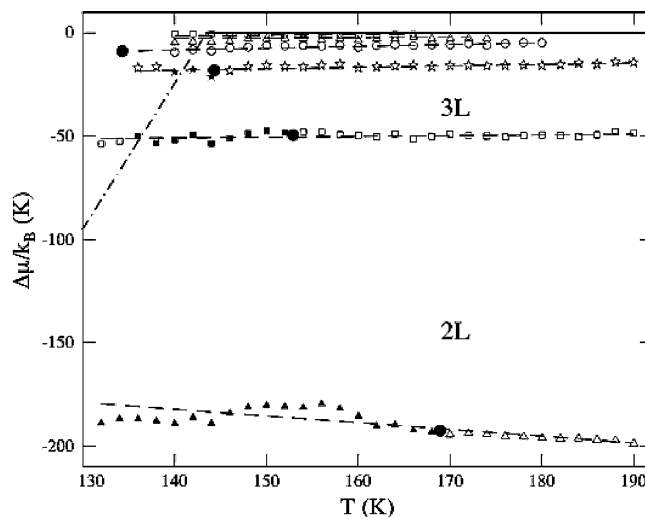


Figure 7. The multilayer μ - T phase diagram. The chemical potential, μ , is measured relative to that of the bulk liquid. The dashed-dotted line is the vapor-solid coexistence line of bulk pentane. Solid symbols correspond to first-order layering transitions; open symbols at higher temperatures, T , correspond to the midpoints of the adsorption steps and represent the continuation of the layering lines into the hypercritical regime. Open symbols above the dashed-dotted line indicate transient, i.e., unstable layers. The solid circles are layer critical points.

fluid monolayer phase. These clusters are actually about 10% denser than the low-temperature crystalline monolayer. In the next section, we will discuss this interpretation in terms of the “footprint reduction” mechanism of melting in alkane monolayers that we have previously proposed.²⁴

IV. Analysis and Discussion

After converting the layering pressures, p_n , into chemical potential differences $\Delta\mu_n = kT \ln(p_n/p_0)$ with respect to the bulk liquid, we plot the resulting μ - T phase diagram in Figure 7. The partial entropy of the second layer is larger than that of the bulk liquid, as is evident from the negative slope of this layering line. The layering lines $n = 3-7$ are parallel to the bulk vapor-liquid coexistence line (vapor pressure line), indicating partial entropies identical to that of the bulk liquid. Therefore, we conclude from the phase diagram in Figure 7 that layers 2-7 are fluid rather than solid.

Although at a temperature of 130 K the first pentane layer is fluid upon its completion, the neutron diffraction results of Arnold et al.²² indicate that it crystallizes as the coverage increases to three layers. They find a crystalline RC structure with lattice constants of $a = 17.1 \text{ Å}$ and $b = 4.26 \text{ Å}$, corresponding to an area per molecule of 36.4 Å^2 . Their structure is compressed about 9% in the b direction from that we measured at monolayer completion at 11 K. Presumably, the upper pentane layers cause this uniaxial compression. Note that their structure has about the same areal density that we have inferred for the monolayer RC clusters at 130 K ($\sim 36 \text{ Å}^2$ per molecule), but the cluster unit cell has a different aspect ratio: $16.0 \text{ Å} \times 4.57 \text{ Å}$.

The presence of clusters in the pentane monolayer fluid having a density higher than the low-temperature crystalline phase may seem unusual, but a similar structure has also been inferred for hexane monolayers on graphite.²⁴ In this case, molecular dynamics simulations showed

(22) Arnold, T.; Dong, C. C.; Thomas, R. K.; Castro, M. A.; Perdigon, A.; Clarke, S. M.; Inaba, A. *Phys. Chem. Chem. Phys.* **2002**, 4, 3430.

(23) Kjems, J. K.; Passell, L.; Taub, H.; Dash, J. G.; Novaco, A. D. *Phys. Rev. B* **1976**, 13, 1446.

(24) Hansen, F. Y.; Taub, H. *Phys. Rev. Lett.* **1992**, 69, 652. Hansen, F. Y.; Newton, J. C.; Taub, H. *J. Chem. Phys.* **1993**, 98, 4128.

patches of solidlike material having an RC structure immersed in a monolayer fluid phase at temperatures just above the monolayer melting point.²⁴ Analysis of neutron diffraction patterns of hexane monolayers indicates the molecular density within these RC patches is 10–20% greater than that found for the low-temperature commensurate HB structure.^{24,25} The hexane molecules in the RC patches as well as in the monolayer fluid in which they are immersed contain a significant number of gauche defects. These molecules have a more globular shape and hence a smaller footprint on the graphite surface, which may explain the higher density of the RC clusters. The smaller footprint of the hexane molecules may also create vacancies within the fluid hexane monolayer, allowing the molecules to rotate more freely and to increase their translational disorder thus stabilizing the fluid phase.

It is of interest to compare the average phase shift per layer measured ellipsometrically $\langle \Delta t_n \rangle$ with the value calculated^{26,27} for different model structures. As a reference case, we take the area per pentane molecule to be 36.6 \AA^2 . This is the value that we have inferred for an RC cluster embedded in the monolayer fluid at 130 K, and here we will assume that it applies to the coexisting fluid as well. We also assume that the molecules are oriented with their long axis parallel to the graphite surface. In addition, we use the isotropically averaged polarizability $\alpha_{av} = 9.95 \text{ \AA}^3$ for the pentane molecule²⁸ and the $\sim 15\%$ anisotropy calculated for the polarizability²⁹ which is in reasonable agreement with gas-phase measurements.³⁰ This model gives $\Delta t_n = 0.392^\circ$ for the phase shift per layer compared to the measured average value $\langle \Delta t_n \rangle = 0.388^\circ \pm 0.002^\circ$. There are a number of uncertainties in the monolayer structure so that this agreement may be fortuitously close. The pentane molecules could be distorted by the presence of gauche defects. This distortion could alter the molecular polarizability or invalidate the assumption that the molecules are lying flat on the surface. Also, the density of the RC clusters may exceed that of the coexisting monolayer fluid. A smaller density would reduce the calculated value of Δt_n .

For comparison, we also calculated Δt_n assuming the pentane molecules to be oriented with their long axis perpendicular to the surface so that the area per molecule was decreased by 28% to 26 \AA^2 . In this orientation, the effective polarizability of the molecule increases by 12%. The higher density and polarizability in this structure yielded $\Delta t_n = 0.55^\circ$ which differs significantly from the measured value of $\langle \Delta t_n \rangle = 0.388^\circ$.

Nham and Hess³ found a negative slope for the second through the sixth layer lines in the μ – T phase diagram of ethane adsorbed on graphite. They attributed a larger entropy in these layers than in the bulk liquid due to reduced constraints on molecular orientation in the fluid film. It seems plausible that this could also be the case for the second pentane layer, although it is not clear why this would not be true for the third through the seventh layers.

We observed layering transitions in our ellipsometric measurements even slightly above the bulk vapor–solid coexistence line (sublimation line) as shown in Figure 7. Such metastable layers persisted over the duration of the

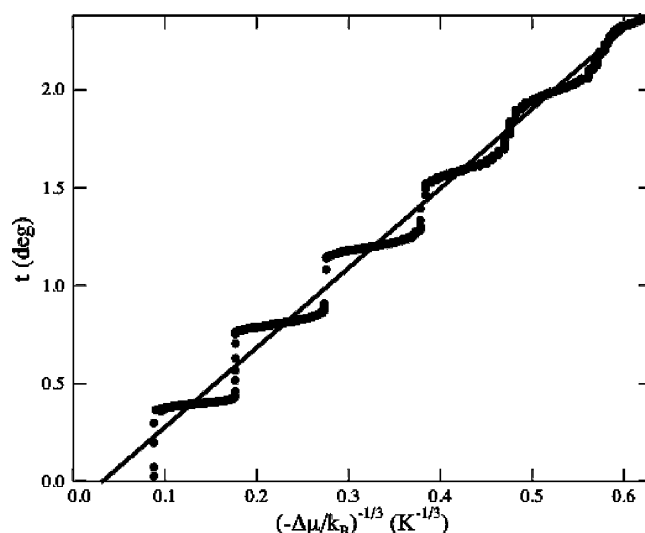


Figure 8. The 154 K isotherm replotted on a $\Delta\mu^{-1/3}$ scale. The solid line is a linear fit to the data points. μ is in units of $k_B T$.

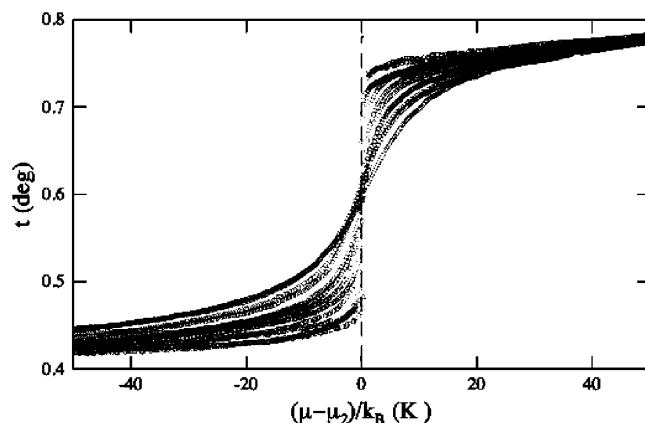


Figure 9. The second step of the isotherms plotted vs μ and shifted in μ such that the step midpoints coincide.

measurements. Layers formed at still higher supersaturations were less stable and disappeared in the course of the measurements.

The Frankel–Halsey–Hill model for multilayer adsorption³¹ states that the sequence of layering pressures, p_n , contains information on the z dependence of the ad molecule–substrate interaction, where z is the distance of the molecule above the adsorbing surface. As shown in Figure 8, the isotherm at a temperature of 154 K can be converted into a series of equidistant steps when the ellipsometric thickness, t , is plotted vs $\Delta\mu^{-1/3}$. This behavior is consistent with a nonretarded van der Waals interaction of the pentane molecules with the substrate atoms and a z^{-3} dependence of the molecule–substrate potential.

The layering steps in t are almost vertical at lower temperatures but become less steep for $T > T_c(n)$. This is illustrated in Figure 9 for $n = 2$ where the second steps in the isotherms at different temperatures are plotted against μ and displaced horizontally so that they coincide at midheight. The slope $d\theta/d\mu$ is just the two-dimensional (2D) compressibility, κ . For a second-order phase transition, κ calculated at midheight should diverge as $[(T - T_c)/T_c]^{-\gamma}$ when approaching the critical point from above. For the 2D Ising model, $\gamma = 7/4$. Adopting the procedure that Nham and Hess applied to ellipsometric measure-

(25) Arnold, T.; Thomas, R. K.; Castro, M. A.; Stuart, S. M.; Messe, L.; Inaba, A. *Phys. Chem. Chem. Phys.* **2002**, *4*, 345.

(26) Shivukin, D. V. *Sov. Phys. JETP* **1956**, *3*, 269.

(27) Dignam, M. J.; Fedyk, J. J. *Phys. (Paris)* **1977**, *38*, C5.

(28) Stuart, H. A. In *Landolt-Börnstein*; Eucken, A., Hellweg, K., Eds.; Springer: Berlin, 1951; sechste Auflage, Vol. I.3, p 512.

(29) Beck, D. R.; Gay, D. H. *J. Chem. Phys.* **1990**, *93*, 7264.

(30) Haverkort, J. E. H.; Baas, F.; Beenakker, J. J. M. *Chem. Phys.* **1983**, *79*, 105.

(31) Frenkel, J. *Kinetic Theory of Liquids*; Clarendon Press: Oxford, 1946. Halsey, G. D., Jr.; *J. Chem. Phys.* **1948**, *16*, 2693. Hill, T. L. *J. Chem. Phys.* **1940**, *17*, 590.

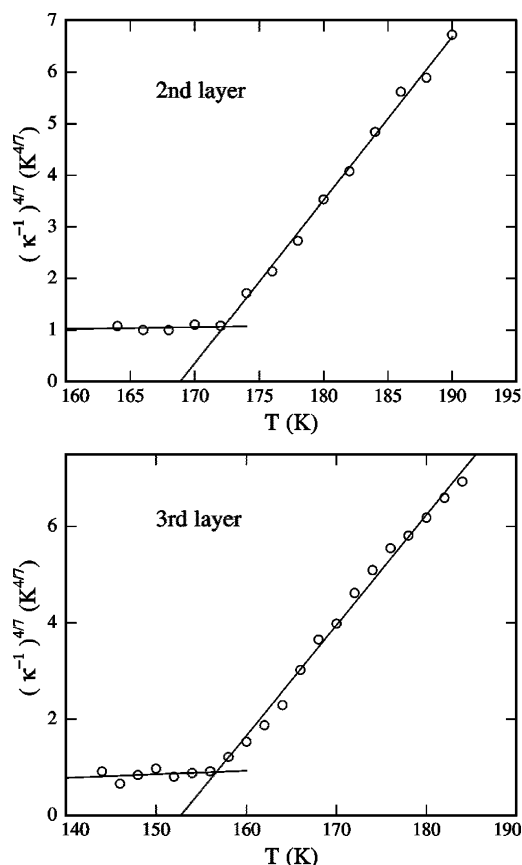


Figure 10. The inverse compressibility of the monolayer steps $n = 2$ and 3 raised to the $4/7$ power and plotted as a function of T .

ments of ethane on graphite,³ we show in Figure 10 plots of $(\kappa^{-1})^{4/7}$ as a function of T for steps $n = 2$ and 3 . The plots are reasonably linear at $T > T_c$, suggesting that the behavior in the hypercritical regime is consistent with the 2D Ising model. The large but finite compressibility at lower temperatures may be due to substrate inhomogeneity and/or a data acquisition too fast to achieve quasiequilibrium.

The critical temperatures $T_c(n)$ are determined from the intersection of the linear section of Figure 10 with the horizontal axis. The T_c for layer $n = 2$ is 168.9 ± 0.3 K. This type of analysis can be extended to layers $n = 3, 4,$

5 , though with decreasing accuracy. Such an analysis gives no indication of a change in critical behavior. We find $T_{c3} = 152.9 \pm 0.45$ K, $T_{c4} = 144.3 \pm 0.8$ K, and $T_{c5} = 134.3 \pm 1.7$ K. The critical point of layer 5 is located above the bulk sublimation line. It is inaccessible under equilibrium conditions.

V. Summary and Conclusions

At monolayer coverage on the graphite basal-plane surface and below a temperature of 99 K, we find that pentane forms a rectangular-centered crystalline structure. Analysis of the temperature dependence of the neutron diffraction patterns supports the footprint reduction melting mechanism previously proposed for alkane monolayers. We interpret the neutron diffraction patterns as indicating dense monolayer clusters coexisting with a monolayer fluid phase in a temperature range of about 30 K above the monolayer melting point. Assuming values of the polarizability tensor from the literature and that the monolayer fluid has the same areal density as that inferred for the coexisting clusters, we calculate an optical thickness of a fluid pentane layer in reasonable agreement with that measured by ellipsometry. Above the bulk triple point, our ellipsometric measurements indicate the growth of at least seven fluid pentane layers of equal optical thickness. In contrast to the growth mode of rare gases on graphite, this layer thickness is independent of layer number up to 190 K. We suggest that this may result from any reduction in molecular density in the higher layers being compensated for by tilting or conformational changes of the molecule that increase its effective molecular polarizability. Analysis of the ellipsometric isotherms shows that growth of the first six fluid layers obeys the Frankel–Halsey–Hill model for multilayer adsorption and that the layering behavior in the hypercritical regime is consistent with a 2D Ising model. Finally, we have determined critical temperatures for layers $n = 2$ – 5 .

Acknowledgment. This work was supported by the Deutsche Forschungsgemeinschaft project Kn 234/9, the U.S. National Science Foundation under Grant Nos. DMR-0109057 and DMR-0411748, the U.S. Department of Energy through Grant No. DE-FG02-01ER45912, the Chilean government under FONDECYT Grant Nos. 1010548 and 7010548, and Fundacion Andes Grant No. C-13768.

LA050338C